Nationaal Lucht- en Ruimtevaartlaboratorium
National Aerospace Laboratory NLR

NLR-TP-98510

Progress Report on Aerodynamic Analysis of a Surface Piercing Hydrofoil-Controlled Wing-In-Ground Effect SEABUS Configuration

C.M. van Beek, B. Oskam and G. Fantacci

Nationaal Lucht- en Ruimtevaartlaboratorium
National Aerospace Laboratory NLR

NLR-TP-98510

Progress Report on Aerodynamic Analysis of a Surface Piercing Hydrofoil-Controlled Wing-In-Ground Effect SEABUS Configuration

C.M. van Beek, B. Oskam and G. Fantacci*

* *Intermarine S.p.A.*

This report is based on a presentation held at the RTO Applied Vehicle Technology Panel Symposium on "Fluid Dynamics Problems of Vehicles Operating near or in the Air-Sea Interface", Amsterdam, 5-8 October 1998.

Division:	Fluid Dynamics
Issued:	November 1998
Classification of title:	unclassified

Contents

(20 pages in total)

PROGRESS REPORT ON AERODYNAMIC ANALYSIS OF A SURFACE PIERCING HYDROFOIL-CONTROLLED WING-IN-GROUND EFFECT SEABUS CONFIGURATION*

C.M. van Beek and B. Oskam
National Aerospace Laboratory NLR
Anthony Fokkerweg 2
1059 CM Amsterdam
The Netherlands

and

G. Fantacci
Intermarine S.p.A.
Via Alta
19038 Sarzana (La Spezia)
Italy

SUMMARY

Preliminary design investigations are presented for a Wing-In-Ground effect craft (SEABUS) in the framework of a European project on technology development for this type of vehicle. The concept of the craft features hydrodynamic control surfaces and a water jet propulsion system.

A computational tool is developed and used to investigate the static equilibrium of lift, drag and pitching moment on the complete configuration over the entire speed range by taking the aerodynamic, hydrodynamic and propulsion contributions into account at the same time. Hydrodynamics turns out to be one of the key factors. At cruise speed the total drag of the presently proposed configuration is dominated by the hydrodynamic contributions of the submerged components.

Limited effort has been spent on the design of the wing and the high lift system. Aerodynamic analysis of this design shows fair correspondence in terms of lift with the required lift values obtained from the preliminary design method. Ground effect trends on performance are correctly calculated. Optimization of the wing and high lift system has to be pursued.

1 INTRODUCTION

Recent industrial needs of shipbuilders and shipoperators are focussed on increasing efficiency and economy of shipping operation. An important aspect in this matter is the speed of the vehicle. Efforts are therefore made worldwide to increase this speed, while keeping safety at an acceptable level. This has led to new concepts for transporters cruising at speeds beyond the limit of conventional high-speed ships. Also improvement has been made of already existing concepts of, for example, hydrofoil boats, hovercrafts, catamarans and trimarans.

One of these new configurations is the Surface Piercing, Hydrofoil-Controlled Wing-In-Ground Effect vehicle. It is basically a large wing operating in ground effect just above the water surface for favourable wing performance; the ground effect increases the lift-drag ratio.

However, flight at an extremely low altitude obviously carries with it a considerable risk, since the time of aerodynamic manoeuvres is relatively large in relation to the short time available at low altitude. The manoeuvrability of the craft is rather limited, since banking in turning operations is hardly possible. A solution to this limitation might be the application of hydrodynamic control through the use of hydrofoils. Due to the much higher density of water compared to air, the response time of the control system is shorter. For the proposed configuration, the hydrofoils are positioned in a trimaran arrangement and are connected to the wing by vertical, water surface piercing struts. An additional aspect is that longitudinal stability of the craft can be obtained by the hydrofoils which implies the redundancy of aerodynamic tail planes.

Separate V-shaped take-off hydrofoils are critical elements of the vehicle to assist in generating lift forces on the configuration and thereby decrease the take-off speed at which the floating hulls of the configuration rise from the water.

In order to continue the development of this concept beyond the conceptual phase, research activities in several technological areas have to be performed in order to obtain a configuration layout which will meet the required control of the craft and also meets the safety regulations. Probably the most important problem to be solved is the cavitation phenomenon on the hydrofoils which occurs at speeds above approximately 40 knots. The availability of hydrofoils for safe and reliable operation in this speed regime is of prime importance for the successful development of the concept.

Intermarine has taken the lead of a European consortium of 13 companies and research institutes to perform research in a number of these areas. The work is performed in the "Brite-Euram III" Programme of the European Commission under the project name SEABUS-HYDAER (HYDrodynamics/AERodynamics); the configuration studied in the project is adopted under the name SEABUS. The project started in December 1997 and will have a duration of 3 years. The main operational requirement of

*The SEABUS configuration is internationally patented by Intermarine S.p.A.; the concept has been established by Admiral Prof.Dr. S. Roccotelli.

the present configuration is to carry 800 passengers and 100 cars at a cruise speed of 120 knots over a distance of 850 km. The emphasis in the present project is on hydrodynamics, aerodynamics and their interaction, on high-speed waterjet propulsion, on the optimization of thick composite structures and on obstacle detection systems.

As project co-ordinator, Intermarine is involved into all aspects of the SEABUS-HYDAER project. As a partner in the project, NLR is involved in the aerodynamics of the wing of the craft. Activities in the aerodynamics field have been defined in the analysis of the wing and its high lift system in ground effect. However, since the performance of the complete vehicle is strongly related to the stability and control of the complete vehicle, it is not meaningful to consider the wing isolated from the hydrodynamic components and the propulsion system. At the start of the project, such an integrated approach has not yet been pursued. Therefore it was imperative to perform a preliminary design study into the controllability of the complete configuration and postpone the detailed wing design until constraints on the wing design goals have been achieved from a preliminary design study.

2 BACKGROUND

From the beginning of the 20th century it was noted that a wing flying in close proximity to the ground experiences an increase of the lift and a reduction of the induced drag. This phenomenon, called ground effect, has been studied since then, because it complicated the take-off and landing of aircraft. Already in 1912 Betz sought to discover what lay behind this phenomenon, see Hooker (Ref. [14]). A historical overview of several projects for Wing-In-Ground (WIG) effect craft until 1980 has been presented by Ollila (Ref. [18]).

Wing-In-Ground (WIG) effect craft have been under development in various countries, such as China, Germany, Italy, Japan, Russia and the United States. From the 1960's Russia put large efforts in the development of "ekranoplans" (Russian for Wing-In-Ground effect vehicles). The central role was played here by Rostislav Alexeyev from the Hydrofoil Design and Construction Bureau. They developed several large ekranoplans (take-off weight from 120 to 550 tonnes). Nowadays there is an extensive amount of open literature available on their research. Examples are: Chubikov et al. (Ref. [6]), Rozhdestvensky (Ref. [21]) and Kirillovikh (Ref. [16]). These papers show that many aspects, such as aerodynamics, propulsion, stability and control, have to be taken into account in close interrelation in order to obtain an efficient transport vehicle. From a United States point of view, the same conclusion was also put forward by Balow et al. (Ref. [3]).

Also smaller scale WIG craft have been developed and built. An example is the work performed by Jörg in Germany since the early 1960's on several small craft (Ref. [15]).

In the future an increasingly important role for WIG craft is envisaged, mainly for civil applications. This prophecy is expressed in many publications, see for example Rozhdestvensky and Synitsin (Ref. [22]). Development of commercial WIG craft is in progress in Russia, Australia, Germany, China and Korea.

A wide variety of techniques have been employed to study the aerodynamics of WIG vehicles. Ando (Ref. [1]) gave a short summary of empirical methods, classical theoretical methods and the Split Orifice Flow Model for the prediction of the lift-to-drag ratio of WIG vehicles. Rozhdestvensky (Ref. [20]) presented one- and two-dimensional mathematical models for the non-linear aerodynamics of lifting surfaces in ground effect. Other methods apply the lifting line theory, matched asymptotic expansions and various implementations of the vortex lattice method, see Hooker (Ref. [14]). A more recent example of the vortex lattice method approach can be found in Day and Doctors (Ref. [9]).

Also panel methods have been used for the calculation of the flow around three-dimensional wings near the water surface. Goetz et al. (Ref. [12]) used the PANAIR panel method for calculations on a low aspect ratio rectangular wing with end plates and trailing edge flap deflection. Chun and Park (Ref. [7]) performed steady and unsteady panel method calculations; the latter showed that the ground effect for a wing above waves is lower than above flat ground. Kühmstedt and Milbradt (Ref. [17]) presented an application of several two- and three-dimensional potential flow methods to the airfoil and wing design of a WIG craft. Chun et al. (Ref. [8]) presented results of panel method calculations not only for wing configurations, but also for a complete WIG craft. Correspondence with experimental results for the wing configurations are shown to be good, except for situations where the wing is in close proximity to the ground. This conclusion has also been drawn in the other panel method references.

With the continuing development and application of Euler and Navier-Stokes codes, these methods have started to be used also in the analysis of WIG configurations; Hirata and Kodama (Ref. [13]) applied a Navier-Stokes solver for calculations on a three-dimensional wing with end-plates in ground effect.

As for cruising conditions, the ground effect plays also an important role at lower speeds in take-off and landing high lift conditions. Steinbach and Jacob (Ref. [23]) conducted a combined experimental and theoretical investigation into a high lift airfoil configuration. They presented the opposite effects of ground influence on lift for two-dimensional airfoils with deflected high lift systems (lift decrease due to the "forward-wash" effect) and for low aspect ratio three-dimensional wings in high lift condition (lift increase due to the image trailing vortices). Filippone and Selig (Ref. [10]) investigated with a panel method the ground effect on a thin and a thick airfoil. They showed opposite effects in extreme ground effect on the thin airfoil (lift increase) and on the thick airfoil (lift decrease). The reason for this is a different balance of the "forward-wash" effect and the "ram" (stagnation) effect. They also studied three-dimensional effects of the flow about low aspect ratio wings by VSAERO panel method calculations; these effects are responsible for the much lower lift coefficients compared to the two-dimensional case.

Most methods for aerodynamic calculations on WIG configurations consider the water surface as not deformable. However, the non-uniform pressure field which is created by the wing, alters the water surface and generates a specific wave pattern. In this sense the aerodynamic flow-field and the hydrodynamic flow-field are strongly coupled. Bulgarelli et al. (Ref. [5]) presented a mathematical model to describe the unsteady flow about a wing moving in the proximity of the air-water interface. As the air-water density ratio is very small, the usual assumption is to neglect completely the free surface deformation and to

consider the WIG craft in flat ground effect. The aerodynamic flow-field and the hydrodynamic flow-field are then assumed to be decoupled.
As already indicated, stability and control of WIG craft is an important aspect which needs careful consideration. Studies into this subject are not as numerous as into the performance of these vehicles. Gera (Ref. [11]) discussed the static and dynamic stability characteristics of wingships.

The present paper presents the status of the limited preliminary design of the complete craft and of the aerodynamic analysis of the wing in ground effect. The next section presents the layout of the configuration, as it is defined at the start of the project by Intermarine. Section 3 deals with the preliminary design investigations. Section 4 shows first results of the wing aerodynamic analysis. Finally, section 5 contains preliminary conclusions on the results obtained up to now.

3 THE SEABUS CONFIGURATION

The initial configuration of the SEABUS has been developed and defined by Intermarine. It is shown in figure 1.

The wing features a low aspect ratio in order to take advantage of the ground effect. The outer parts of the wing can be folded to reduce the span for manoeuvring operations in harbours. The high lift system of the wing consists of a full-span trailing edge single-slotted Fowler flap. Passengers and cargo are accommodated inside the inner part of the wing. The absence of a fuselage is favourable for achieving a high lift/drag ratio of the configuration.
Three hulls are connected in a trimaran configuration to the lower surface of the wing; one hull in a forward position in the plane of symmetry, the two others in an aft starboard and port position. The main purpose of the three hulls is to provide buoyancy during floating operations at low speed in harbours and in take-off and re-entry operations.

The complete speed range is subdivided into three subranges:

- the planing hull state or the hullborne state (0-30 knots)
- the foilborne state (30-70 knots)
- the airborne state (70-120 knots)

The speed between hullborne state and foilborne state is defined as the take-off speed. The speed between foilborne state and airborne state is defined as the minimum airborne speed.

The SEABUS features a set of V-shaped take-off hydrofoils which is separate from the control hydrofoils. The V-shaped take-off foils generate additional lift in the foilborne state of the flight between the take-off and the airborne state, i.e. the operation state where the weight of the craft is fully carried by the wing. These take-off foils are partially submerged in the foilborne state and are above the water in the airborne state.

Control hydrofoils are used for longitudinal controllability of the craft in the foilborne and airborne state. These control foils are non-movable and do not feature flaps. Control is accomplished by the blowing of air from the upper or lower side of the foils at the mid-chord location.

The take-off foils are vertically positioned in such a way that they are fully submerged in the planing hull state in order to generate maximum lift to decrease the take-off velocity as far as possible. Applying take-off hydrofoils will allow the take-off at a lower speed than in case the configuration only features an aerodynamic wing to generate lift. After take-off the vehicle rises with increasing speed due to the lift force generated by the take-off hydrofoils and the wing, such that just after take-off the hulls are already well above the surface surface. Also the V-shaped take-off foils become decreasingly submerged with increasing speed. At the speed where the vehicle becomes fully airborne the take-off foils are no longer submerged, therefore not contributing to the hydrodynamic drag in the airborne speed regime. The control foils are located at the bottom of the struts and remain submerged over the entire speed range of the craft.
An example of an existing WIG craft with hydrofoils is the Lippisch X-114H.
Propulsion of the vehicle is provided by a waterjet, located just under the wing at the end of the front hull. The water jet nozzle can be tilted from a horizontal position towards a 10 degrees downward position. In this way the thrust can also assist in the generation of the required lift force during take-off. The water inlet is located at the bottom of the front strut. The inlet duct runs through this strut upwards to the pump which is located in the front hull. The thrust is generated by a gas-turbine, also placed inside this hull, which is connected by a gearbox to the pump.
The main characteristics of the SEABUS configuration are:

- weight:
  - take-off: W_{to} = 500 ton
  - payload: W_p = 266.5 ton
- cruise speed: U_∞ = 120 kts
- wing:
  - span: b = 111.92 m
  - mean aerodynamic chord: $\bar{c}$ = 48.64 m
  - taper ratio: λ = 0.5
  - aspect ratio: A = 2.38
  - area: S = 5254 m^2
  - non-dimensional span of prismoidal center section: b_{pr}/b = 0.4465
  - dihedral angle of outer wing part: Γ = 5.22°
  - straight quarter-chord line
- front strut:
  - 30 % thick, base vented, parabolic profile
  - span: b = 7.60 m
  - chord: c = 4.70 m
  - forward sweep angle: Λ = 30°

- aft strut:
  - 20 % thick, base vented, parabolic profile
  - span: b = 7.40 m
  - chord: c = 3.33 m
  - sweep angle: Λ = 0 °
- front take-off hydrofoil:
  - 6 % thick, base vented, curved, parabolic profile
  - straight-tapered, taper ratio: λ = 0.5
  - aspect ratio: A = 8.26
  - area: S = 40 m^2
  - V-shaped, dihedral angle: Γ = 30 °
- front control hydrofoil:
  - 6 % thick, NACA 16006 profile
  - airfeed at 50 % chord on the upper and lower side, for lift variation for control purposes ($\Delta c_{l_{profile}}$=±0.15)
  - straight-tapered, taper ratio: λ = 0.39
  - aspect ratio: A = 5.36
  - area: S = 10 m^2

The two aft take-off hydrofoils feature each only half of the front take-off hydrofoil: at the starboard-side aft strut only the starboard-side of the front foil, S = 20 m^2, at the port-side aft strut only the port-side of the front foil, S = 20 m^2. Each of the two aft control hydrofoils features half of the front control hydrofoil area: S = 5 m^2, at the same values of the other foil parameters.
In summary we have:

- total take-off foil area: 40+20+20=80 m^2
- total control foil area: 10+5+5=20 m^2

4 THE PRELIMINARY DESIGN CALCULATIONS

A limited preliminary design for the SEABUS configuration has been performed. The aim was to determine the performance of the vehicle and the amount of propulsive power required for obtaining static equilibrium with regard to lift, drag and pitching moment. Also it has to provide the design lift coefficients for the wing, the wing pitching moment limitations in both cruise and high lift configurations and the angle of attack limitations, which will be used in the detailed design of the wing and the high lift system of the wing. This section presents several aspects of the preliminary design and results of calculations.

4.1 Aspects of the preliminary design

The lift and drag data over the entire speed range for the hydrodynamic components of the SEABUS configuration are provided to NLR by the partners in the SEABUS-HYDAER consortium which are responsible for the design, testing and validation of the hulls, struts, take-off foils and control foils. Data on the propulsion (water inlet and water jet) has also been supplied to NLR by the partner responsible for this subject. These data itself are not discussed in the present paper. It has to be realized that these data are a first iteration. The hydrodynamic behaviour of struts and foils at the speed range in which the SEABUS is intended to operate is an unknown area in which super-cavitation phenomena play a dominant role. It is exactly one of the goals of the present project to obtain hydrodynamic data up to speeds of 120 knots. The same holds for the propulsion; the flow in the inlet at high velocities is also strongly infuenced by cavitation. This will also be investigated in the project.
The aerodynamic characteristics of the wing and the high lift system are calculated with well-established preliminary design methods, taken from Ref. [24]. It also includes corrections for the lift, drag and pitching moment due to the ground effect. The effect of the deformable water surface has not been taken into account.

Beside the geometrical data already discussed, a number of additional data has also to be defined to perform the static analysis. The wing profile characteristics are defined in such a way that, at the cruise speed of 120 kts, the wing lift for zero angle of attack, plus the component in lift direction of the pressure related part of the force on the water inlet, equal the weight of the craft. The inlet features an inclination angle of 30 degrees with respect to the vertical axis. The wing lift coefficient in cruise equals: $C_{L_{wing_{cruise}}}$ = 0.39. The wing planform, as specified in the previous section, has been used. The flap/wing chord ratio has been selected at 0.35. No attempts have been made to optimize this ratio. The center of gravity and its range are defined; the average location is at 30 % of the wing root chord from the leading edge.
The height of the wing above the water surface and its angle of attack depend on the phase of the flight. From zero up to take-off speed the craft is in the planing hull state where it is planing on the three hulls. The height above the surface is selected at 2.4 meter. In the foilborne state from the take-off velocity up to the fully airborne velocity the height increases with increasing speed. The height is determined by the extent of submergence of the take-off hydrofoils which is required to generate, in combination with the lift on the wing, the total lift on the vehicle. The total lift equals the weight of the configuration. Therefore the height in the foilborne state results from the calculations. In the airborne state the height is defined at 9 meter, such that the take-off foils are above the water surface. This implies that the craft is flying at a relative flight height of 18.5 % of the mean aerodynamic chord length. A wing with an aspect ratio between 2 and 3, flying at a relative flight height of 20 % of the mean aerodynamic chord length is considered acceptable for an efficient transport vehicle, see Kirillovikh (Ref. [16]). Rozhdestvensky (Ref. [20]) states that the relative ground clearance should be in the range of 5-10 % of the mean chord for obtaining efficient WIG craft from the viewpoint of aerodynamics. The seastate (waveheight) comes also into the picture, requiring a larger percentage.
The minimum take-off velocity is determined by the condition that the take-off hydrofoils and the wing carry the vehicle (the front and two aft control foils together are assumed to generate no net lift); the value of this velocity is therefore a result from the calculations. The minimum airborne velocity is determined by the condition that the wing fully carries the vehicle; the value of this velocity is also a result from the calculations.

Finally, the angle of attack of the craft in the planing hull state and the foilborne state can only be chosen within strict limits. Restrictions are the requirements that the wing trailing edge does not touch the water surface and that the water inlet and, at the take-off velocity, the take-off foils remain properly submerged. A limited angle is also a requirement to avoid shifting of the cars in the cargo-space, since it will be in practice impossible to fasten all cars sufficiently to the floor. In the present preliminary design calculations the angle of attack has been set at zero degrees. In the airborne state the angle of attack results from the analysis by the condition that at all speeds in this state the wing generates a lift force which equals the weight of the vehicle.

The hydrodynamic, propulsion, aerodynamic and additional data are combined in a computer program in order to calculate the performance over the entire velocity range, for minimum required power, of the complete vehicle based on static equilibrium of the lift, drag and pitching moment, i.e. only starboard/port-side symmetric conditions are considered. All calculations are made for the take-off weight of the vehicle and for the average location of the center of gravity.

4.2 Results of preliminary design calculations

Calculations have been performed in order to establish the inputs for the detailed aerodynamic design of the SEABUS configuration. The results of the calculations are summarized for a number of velocities in the tables 3 and 4.

The take-off velocity is 30 knots; the presently calculated minimum airborne velocity is 70 kts. At the latter speed the vehicle can change the foilborne state into the airborne state by simultaneously increasing the height above the water surface and increasing the angle of attack. After take-off the increased height above the water surface enables to deflect the wing trailing edge flap to 10 degrees, and above 45 knots to 15 degrees.

In the foilborne state the lift force on the take-off hydrofoils decrease with increasing speed, while the wing increasingly takes over the function of lift generation device. This is also presented in Fig. 2 in which the total lift coefficient of the vehicle for static equilibrium is plotted; also shown are the lift coefficient of the take-off hydrofoils (front and two aft together) and the wing. All coefficients are based on the dynamic pressure of the airflow and the planform area of the wing (to allow addition).

Figure 3 presents the lift coefficient of the wing and the angle of attack over the speed range; also the trailing edge flap deflection angles are indicated. In the planing hull and foilborne state the angle of attack has to remain zero degrees. In the airborne state the angle of attack varies with speed in order to achieve at all speeds equilibrium of forces and pitching moment, while fluctuations of the flap deflection angle, which is at its maximum of 15 degrees at 70 kts, are avoided, such that the flap can be retracted smoothly with increasing speed until the high lift system is no longer required at 100 kts.

Table 4 shows the drag on the components and on the entire configuration. Clearly the hydrodynamic components account for the largest portion of the drag. The drag contribution of the wing is 15 per cent at 120 knots. This is also illustrated in Fig. 4 where the drag of the various components is given as percentage of the drag of the entire vehicle.

Fig. 5 presents the installed power over the speed range. As for "conventional" WIG craft, the power required reaches a local maximum at the take-off speed due to the wave-making drag of the hulls which are no longer submerged in the foilborne state. In the foilborne state the power required is nearly constant, because the hydrodynamically wetted area decreases with in creasing speed due to the increased height of the vehicle above the water surface. As shown in Table 4, the drag of the configuration decreases in the foilborne state with a factor two, while the speed doubles from 35 to 70 knots. In the airborne speed range, being at a constant height of 9 meter, the power required approximately increases up to the overall maximum of 90 MegaWatt at 120 kts. This is in contrast to conventional WIG craft without submerged components above the take-off speed for which the overall maximum power required is determined by the wave-making drag at the take-off speed.

The high value of the maximum installed power required affects the operational efficiency in an adverse way. Ando (Ref. [2]) devised the non-dimensional "Modified Effective Lift-Drag Ratio" parameter: $(WV/P)M_{cr}$, where W is the weight, V the cruise velocity, P the installed power and M_{cr} the Mach number at cruise. Ando presented plots for this parameter based on the gross-weight W_g and on the payload W_p for a wide range of transport vehicles. For the present SEABUS configuration the numbers are: W_g = 500 ton (gross-weight), W_p = 266.5 ton (payload), V_{cr} = 120 kts, P_{in} = $\pm$90 $MegaWatt$ and M_{cr} = 0.18. These data result in two values of the efficiency parameter $(WV/P)M_{cr}$:

1. one based on gross-weight; this value of the SEABUS configuration equals the value for an efficient helicopter in comparison with various other transport vehicles, as presented by Ando.

2. one based on payload; this value of the SEABUS configuration exceeds that of helicopters, and equals the value for a passenger car and, although operating in a higher speed range, the value for less efficient jet aircraft.

5 THE DETAILED DESIGN CALCULATIONS

Detailed wing design activities have recently been started. This section describes the work performed on the wing profile and trailing edge flap profile design and on the analysis of the performance of the three-dimensional wing and the high lift system.

5.1 Wing and flap profile design

Recently, detailed analysis of the performance of the wing has been started. Based on the lift coefficients for the wing, obtained from the preliminary design calculations, wing profile design can be performed. Initially, Intermarine has chosen the Göttingen 1020 profile for the SEABUS wing. A first iteration in this profile design has been executed. Using a two-dimensional panel method with ground effect capability, coupled with a boundary layer method, see Ref. [19], a profile with enhanced lift capability has been designed during an earlier design iteration, allowing for larger angles of attack up to seven degrees. Modifications to the original profile relate to the upper side near the nose and the adoption of a flat lower side, see Fig. 6, where the profiles are shown at airborne height.

The trailing edge flap profile is based on the single-slotted flap of a three element airfoil. The flap/wing chord ratio is 0.35. The geometry of the flap has been modified in order to integrate it in

retracted position smoothly in the wing profile. The flap/wing chord ratio has been kept the same. Fig. 7 shows the flap profile in retracted and deflected position at a foilborne height.
Since wing analysis is performed with a non-viscous potential flow method, a modification to the wing profile with relation to the flap cove has to be made in case of calculations on the wing with deflected flap in order to prevent unrealistic results in the cove. To simulate flow separation in the potential flow calculations, the cove has been faired smoothly from the profile lower side to the trailing edge, see Fig. 7.
It is mentioned that the two-dimensional wing and flap profile design, which has been performed up to now, is of limited scope. Complete wing design activities would require several iteration loops of preliminary design calculations, as presented in the previous section, two-dimensional profile design and three-dimensional detailed design, as is presented in the next subsection.

5.2 Wing-In-Ground effect calculations

A number of aerodynamic calculations on the SEABUS wing have been performed. The calculational method is the PDAERO panel method, see Ref. [4]. This method is capable of the calculation of the three-dimensional inviscid, subsonic potential flow on arbitrary aeronautical configurations. The method includes an option for (undeformable) ground effect calculations.
The geometry of the wing is based on the planform which has been defined by Intermarine and which is presented in section 2. The wing and flap profile are discussed in section 4.1. The flap/wing chord ratio is constant in spanwise direction.
Calculations have been performed at one foilborne and two airborne conditions (all conditions are starboard/port-side symmetric):

1. U_∞ = 50 kts, α = 0°, δ_f = 15°
2. U_∞ = 85 kts, α = 2.1°, δ_f = 5°
3. U_∞ = 120 kts, α = 0°, δ_f = 0°

The full-span, single-slotted trailing edge flap is of the Fowler type. The chord extension due to the translation of the flap in backward direction is set at 30 % flap chord at 5° flap deflection and at 50 % flap chord at 15° flap deflection. The extension percentages are constant in spanwise direction. For both deflection angles, the gap between wing and flap is 2 per cent of the wing chord without flap deflection, again constant in spanwise direction.
The panel distribution is shown in Fig. 8 and 9 for the wing with retracted flap and in Fig. 10 for the wing with flap deflection. Fig. 11 shows details of the wing and flap paneling, including their wakes, near the wing trailing edge. The wake of the main wing, trailing off in downstream direction over the deflected flap, is taken parallel to the upper surface of the flap up to the trailing edge of the flap.
At each condition calculations have been performed with and without ground effect in order to investigate this phenomenon.
The number of panels for the clean wing geometry is: 2700 (in ground effect effectively 5400), for the wing with deflected flap: 4500 (in ground effect effectively 9000). The calculations have been executed on the NEC SX-4 supercomputer of NLR. Run times vary from 55 seconds for the clean wing without ground effect calculation to 250 seconds for the calculation on the wing with deflected flap including ground effect.

	$h[m]$	$U_\infty[kts]$	$\alpha[°]$	$\delta_f[°]$	C_L	C_D	L/D
1a	∞	50	0	15	0.8376	0.0300	28
1b	6.15	50	0	15	1.2668	0.0156	81
2a	∞	85	2.1	5	0.5705	0.0267	21
2b	9	85	2.1	5	0.7803	0.0165	47
3a	∞	120	0.1	0	0.2780	0.0160	17
3b	9	120	0.1	0	0.3939	0.0104	38

Table 1: Wing lift and wing drag coefficents at three conditions from the preliminary design calculations

	$h[m]$	$U_\infty[kts]$	$\alpha[°]$	$\delta_f[°]$	C_L	C_{D_i}	L/D_i
1a	∞	50	0	15	0.8357	0.0900	9
1b	6.15	50	0	15	1.4511	0.0670	22
2a	∞	85	2.1	5	0.5971	0.0460	13
2b	9	85	2.1	5	0.9055	0.0429	21
3a	∞	120	0	0	0.3027	0.0119	25
3b	9	120	0	0	0.3824	0.0093	41

Table 2: Wing lift and wing induced drag coefficents at three conditions from the PDAERO calculations

Pressure distributions over the wing and flap, for two spanwise locations (η=$y/(b/2)$ = 0.2 and 0.7) and spanwise lift distributions are presented in Fig. 12 through 19. At all conditions, the ground effect increases the pressure at the lower side of the wing, while the distribution at the upper side remains relatively unchanged. The ground effect is most prominent at the foilborne condition where the wing is closest to the ground.
The results for lift and drag are given in table 1 and 2. Table 1 contains the lift and total drag from the preliminary design calculations, table 2 the lift and induced drag from the PDAERO calculations. In both tables results without and with ground effect are presented. Comparison of lift coefficients shows that without ground effect the lift values are in fair correspondence. With ground effect larger differences occur for the two high lift conditions.
Comparison of drag coefficients shows that the panel method values, consisting of induced drag only, are higher than the values resulting from the preliminary design calculations in the two high lift conditions, but lower at cruise condition.
These wing analysis results should be regarded as results in progress for the SEABUS configuration. The generally fair correspondence between the results on lift from the preliminary design calculations and from the wing analysis indicate that the wing design can be developed further from the present layout. Design of the wing and the high lift system (flap gap and overlap) is possible through modification of several parameters, such as wing leading edge curvature, which define a complete, three-dimensional wing.

6 CONCLUSIONS

A description has been presented of a preliminary design investigation into the SEABUS WIG concept which features hydrodynamic control surfaces and a water jet propulsion system.
A computational tool has been developed allowing to calculate static equilibrium states with relation to lift, drag and pitching

moment in a rapid manner, taking severe operational limitations in terms of the angle of attack into account. The preliminary design results indicate a drag level dominated by hydrodynamic contributions and as a consequence a large installed power. The resulting operational efficiency of the SEABUS, based on gross-weight, equals the value of efficient helicopters; the operational efficiency of the SEABUS, based on payload, equals the value of passenger cars and, although operating in a higher speed range, the value of less efficient jet aircraft. These efficiencies indicate the need for further design iterations to reduce the hydrodynamic drag level of the SEABUS concept, by reducing the size of the struts and the control foils, to increase the operational efficiency.

7 REFERENCES

[1] Ando, S., "Note on Prediction of Aerodynamic Lift/Drag Ratio of WIG (Wing-In-Ground) at Cruise", Proc. of FAST'93, Yokohama, Japan, Dec. 13-16, 1993, pp. 1561-1572.

[2] Ando, S., "Some Topics on WIG (Ekranoplan) Design", Trans. of the Japan Society for Aeronautical and Space Sciences, Vol. 39, No. 124, Aug. 1996, pp. 184-198.

[3] Balow, F.A., Guglielmo, J.G. and Sivier, K.R., "Design and Evaluation of a Midsize Wing-in-Ground Effect Transport", AIAA 93-3952, AIAA Aircraft Design, Systems and Operations Meeting, Monterey, CA, Aug. 11-13, 1993.

[4] Beek, C.M. van, Piers, W.J. and Oskam, B., "Aerodynamic Analysis of Slipstream/Wing/Nacelle Interference for Preliminary Design of Aircraft Configurations", AGARD-CP-498, Paper No. 6, 1992.

[5] Bulgarelli, U.P., Greco, M., Landrini, M. and Lugni, C., "A Simple Model for the Aero-Hydrodynamics of Ekranoplans", Proc. of the AGARD Fluid Dynamics Panel Workshop on High Speed Body Motion in Water, Kiev, Ukraine, Sept. 1-3, 1997, AGARD-R-827, Paper 16.

[6] Chubikov, V., Pashin, V., Treschchevsky, V. and Maskalik, A., "Ekranoplan: A High-Speed Marine Vehicle of a New Type", Proc. of FAST'91, Vol. 1, June 1991, pp. 641-648.

[7] Chun, H.H. and Park, I.R., "Analysis of Steady and Unsteady Performances for 3-D Airwings in the Vicinity of the Free Surface", Proc. of a Workshop on Twenty-First Century Flying Ships, Sydney, Australia, Nov. 7-8, 1995, pp. 23-46.

[8] Chun, H.H., Park, I.R., Chung, K.H. and Shin, M.S., "Computational and Experimental Studies on Wings In Ground Effect and a WIG Effect Craft", Workshop Proc. of Ekranoplans and Very Fast Craft, Sydney, Australia, Dec. 5-6, 1996, pp. 38-59.

[9] Day, A.H. and Doctors, L.J., "A Study on the Efficiency of the WIG Concept", Proc. of a Workshop on Twenty-First Century Flying Ships, Sydney, Australia, Nov. 7-8, 1995, pp. 1-22.

[10] Filippone, A. and Selig, M.S., "Low Aspect-Ratio Wings for Wing-Ships", AIAA 98-0761, 36th Aerospace Sciences Meeting and Exhibit, Reno, NV, Jan. 12-15, 1998.

[11] Gera, J., "Stability and Control of Wing-In-Ground Effect Vehicles or Wingships", AIAA 95-0339, 33rd Aerospace Sciences Meeting and Exhibit, Reno, NV, Jan. 9-12, 1995.

[12] Goetz, A.R., Osborn, R.F. and Smith, M.L., "Wing-In-Ground Effect Aerodynamic Predictions Using PANAIR", AIAA-84-2429, AIAA Aircraft design systems and operations meeting, San Diego, CA, Oct. 31 - Nov. 2, 1984.

[13] Hirata, N. and Kodama,Y., "Flow Computation for Three-Dimensional Wing in Ground Effect Using Multi-Block Technique", Journal of the Society of Naval Architects of Japan, Vol. 177, June 1995. pp. 49-57.

[14] Hooker, S.F., "A Review of Current Technical Knowledge Necessary to Develop Large Scale Wing-In-Surface Effect Craft", Intersociety Advanced Marine Vehicles Conf., Arlington, VA, June 5-7, 1989, pp. 367-429.

[15] Jörg, G.W., "History and Development of the "Aerodynamic Ground Effect Craft" (AGEC) with tandem wings", Proc. of the Symposium "Ram Wing and Ground Effect Craft", The Royal Aeronautical Society, London, England, May 19, 1987, pp. 87-109.

[16] Kirillovikh, V.N., "Russian Ekranoplans", Proc. of a Workshop on Twenty-First Century Flying Ships, Sydney, Australia, Nov. 7-8, 1995, pp. 71-117.

[17] Kühmstedt, T. and Milbradt, G., "Aerodynamic Design of Wing in Ground Effect Craft", Proc. of FAST'95, Lübeck-Travemünde, Germany, Sept. 25-27, 1995, Vol. 1, pp. 597-608.

[18] Ollila, R.G., "Historical Review of WIG vehicles", Journal of Hydronautics, Vol. 14, No. 3, July 1980, pp.65-76.

[19] Oskam, B., Laan, D.J. and Volkers, D.F., "Recent Advances in Computational Methods to Solve the High-Lift Multi-Component Airfoil Problem", AGARD-CP-365, Paper No. 3, 1984; also NLR MP 84042 U, 1984.

[20] Rozhdestvensky, K.V., "Nonlinear Aerodynamics of Ekranoplan in Strong Ground Effect", Proc. of FAST'95, Lübeck-Travemünde, Germany, Sept. 25-27, 1995, Vol. 1, pp. 621-630.

[21] Rozhdestvensky, K.V., "Ekranoplans - Flying Ships of the Next Century", Proc. of a Workshop on Twenty-First Century Flying Ships, Sydney, Australia, Nov. 7-8, 1995, pp. 47-70.

[22] Rozhdestvensky, K.V. and Synitsyn, D.N., "State-of-the-Art and Perspectives of Development of Ekranoplans in Russia", Proc. of FAST'93, Yokohama, Japan, Dec. 13-16, 1993 pp. 1567-1670.

[23] Steinbach, D. and Jacob, K., "Some Aerodynamic Aspects of Wings near Ground", Trans. of the Japan Society for Aeronautical and Space Sciences, Vol. 34, No. 104, Aug. 1991, pp. 56-70.

[24] Torenbeek, E., "Synthesis of Subsonic Airplane Design", Delft University Press and Martinus Nijhoff Publishers, 1982.

W = vehicle weight

SEABUS - lift force											
	h	hulls		take-off foils		wing					
U_∞	α=0	lift force		lift force		lift force			α	δ_f	
$[kts]$	$[m]$	$[ton]$	$\%\,W$	$[ton]$	$\%\,W$	$[ton]$	$\%\,W$	$C_{L_{wing}}$	$[deg]$	$[deg]$	state
0	2.40	500	100.0	0	0	0	0	0	0	0	hullborne
10	2.40	438.4	87.7	43.6	8.7	7.0	1.4	0.8066	0	0	hullborne
20	2.40	291.4	58.3	174.3	34.9	28.0	5.6	0.8066	0	0	hullborne
30	2.40	46.3	9.3	392.1	78.4	62.9	12.6	0.8066	0	0	hullborne
35	4.24	0	0	364.9	73.0	135.1	27.0	1.2698	0	10	foilborne
40	5.00	0	0	340.2	68.0	159.8	32.0	1.1517	0	10	foilborne
50	6.15	0	0	223.5	44.7	276.5	55.3	1.2668	0	15	foilborne
60	6.88	0	0	116.9	23.4	383.1	76.6	1.2092	0	15	foilborne
70	7.86	0	0	3.0	0.6	496.9	99.4	1.1523	0	15	foilborne
70	9.00	0	0	0	0	490.9	98.2	1.1560	0.8	15	airborne
80	9.00	0	0	0	0	491.0	98.2	0.8853	0.6	9	airborne
90	9.00	0	0	0	0	490.4	98.1	0.6986	0.8	5	airborne
100	9.00	0	0	0	0	485.5	97.1	0.5602	2.6	0	airborne
110	9.00	0	0	0	0	488.6	97.7	0.4659	1.1	0	airborne
120	9.00	0	0	0	0	491.5	98.3	0.3939	0.1	0	airborne

Table 3: *Lift force distribution*

SEABUS - drag force							
	hulls	struts	take-off foils	control foils	wing	conf.	
U_∞	drag	drag	drag	drag	drag	drag	
$[kts]$	$[kg]$	$[kg]$	$[kg]$	$[kg]$	$[kg]$	$[kg]$	state
0	0	0	0	0	0	0	hullborne
10	7000	125044	1292	1858	90	135283	hullborne
20	20000	127435	5168	7336	354	160293	hullborne
30	51000	131087	11630	16394	788	210898	hullborne
35	0	87696	13653	22260	1464	125073	foilborne
40	0	73450	15051	24085	1816	114402	foilborne
50	0	55415	13073	23935	3379	95802	foilborne
60	0	46794	7944	24531	5177	84446	foilborne
70	0	35309	300	25041	7599	68249	foilborne
70	0	22302	0	23535	8800	54637	airborne
80	0	24384	0	25360	9070	58813	airborne
90	0	28004	0	27437	9545	64986	airborne
100	0	37170	0	28101	14201	79473	airborne
110	0	35980	0	28712	13324	78016	airborne
120	0	36241	0	35276	12997	84513	airborne

Table 4: *Drag force distribution*

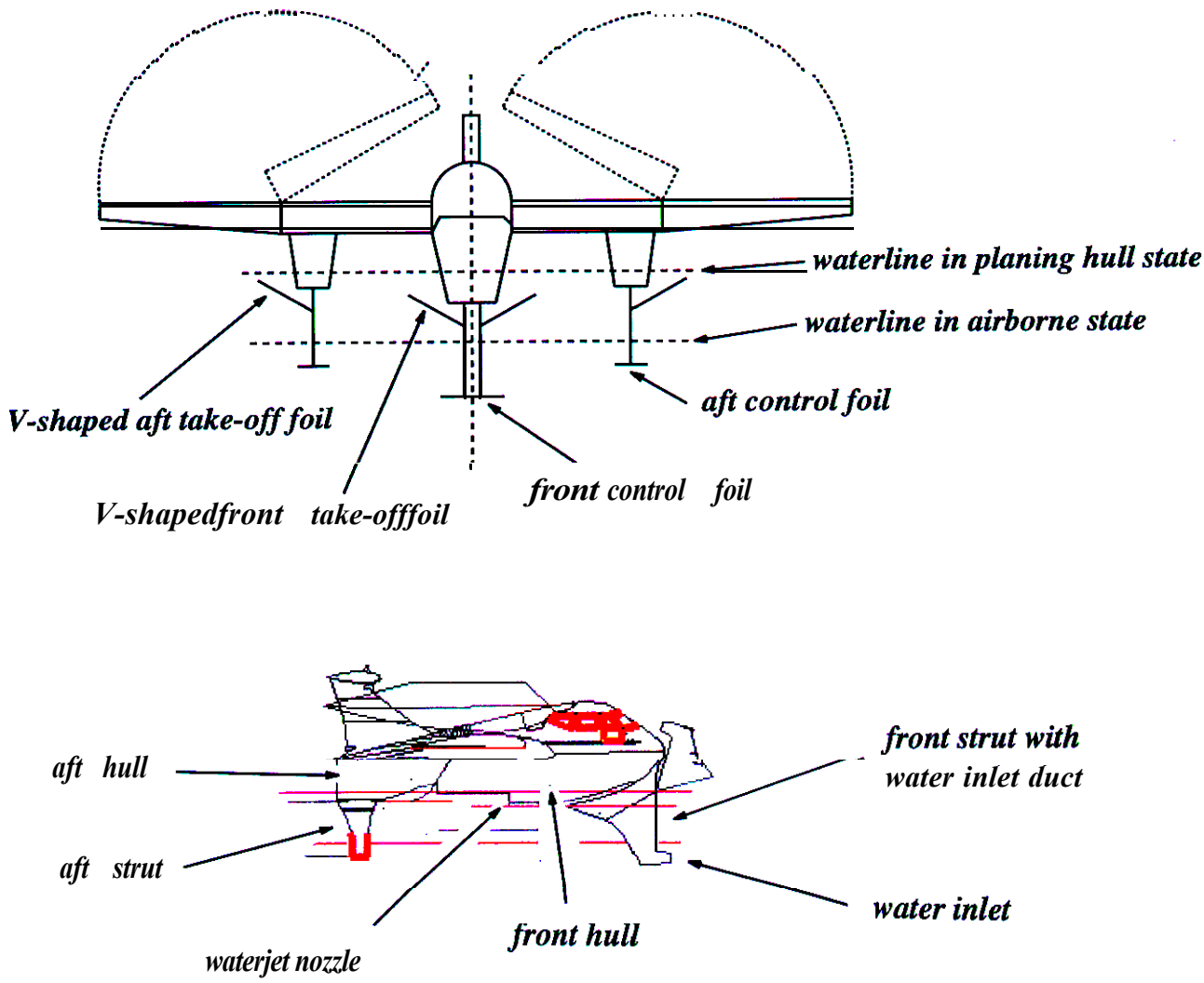

Figure 1: *The SEABUS configuration (on scale of the Technology Demonstrator)*

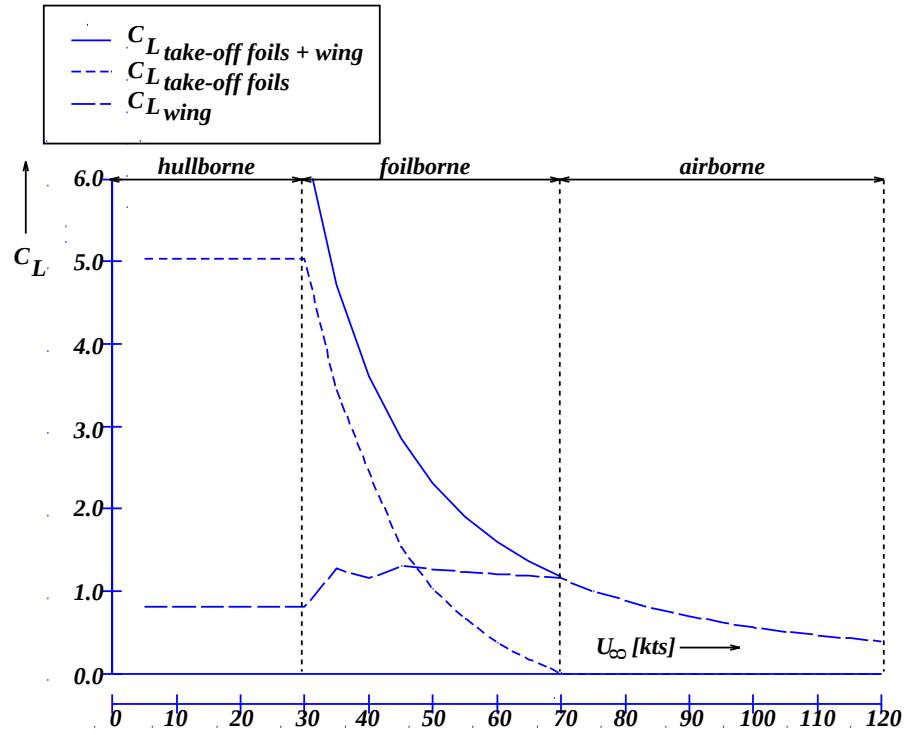

Figure 2: *Lift coefficients for static equilibrium over the speed range*

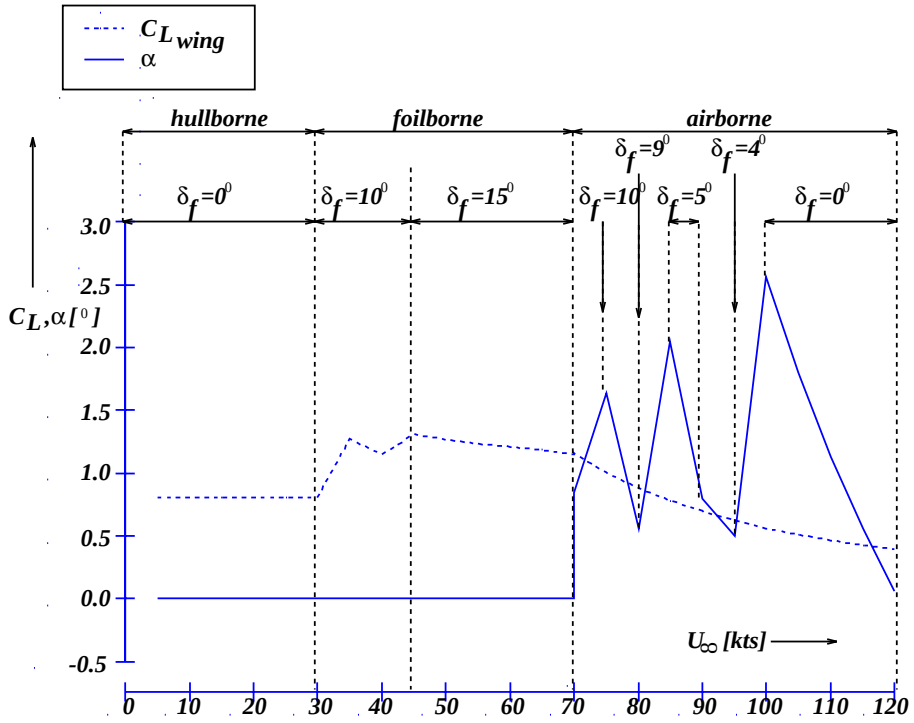

Figure 3: *Wing lift coefficient and angle of attack for static equilibrium over the speed range*

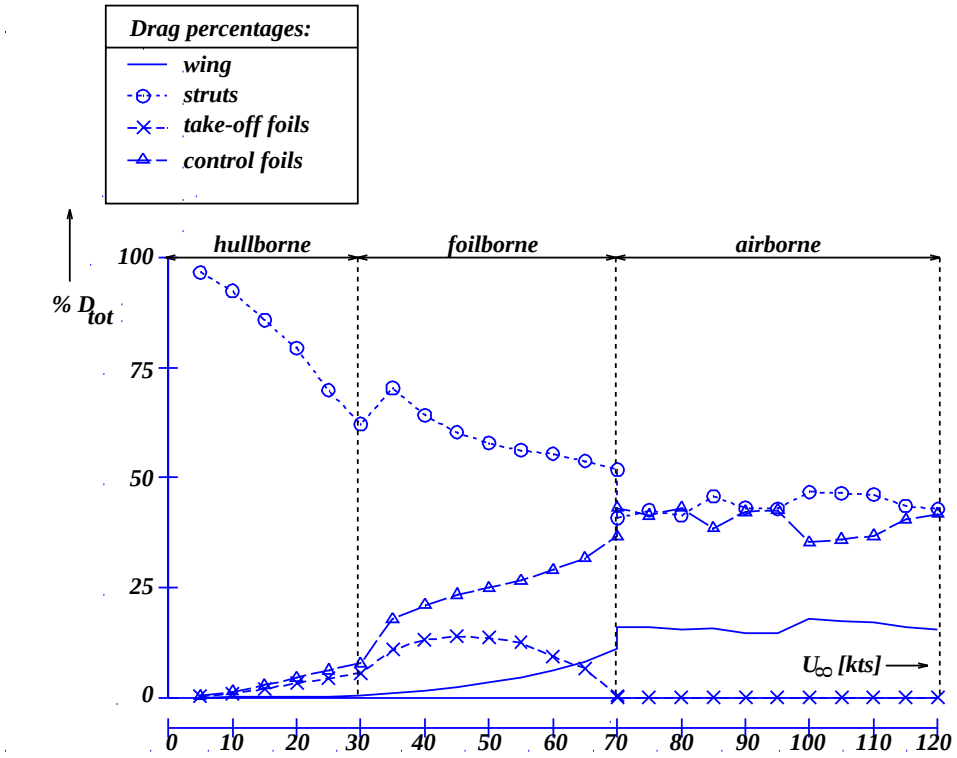

Figure 4: *Drag of various configuration components as percentage of the total drag at static equilibrium over the speed range*

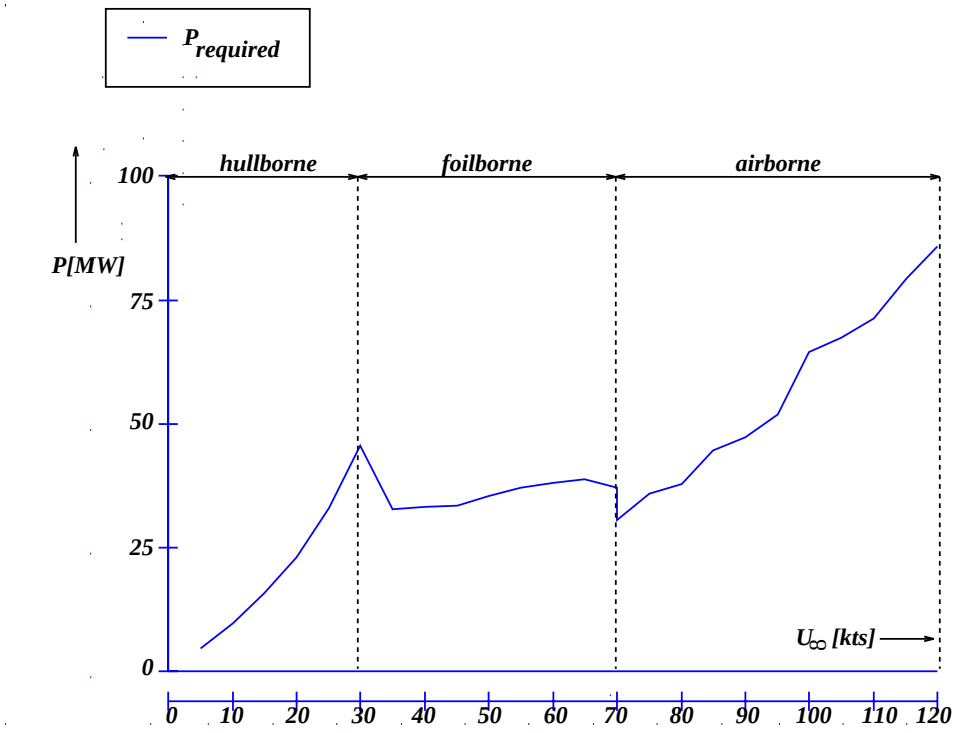

Figure 5: *Installed power required at static equilibrium (lift, drag and pitching moment) over the speed range*

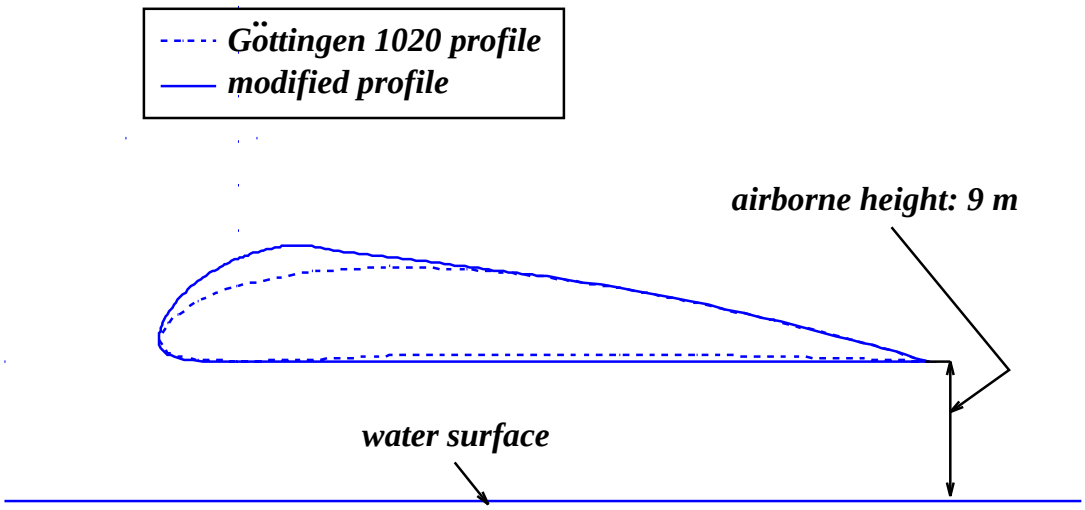

Figure 6: *The initial and modified wing profile (of earlier design iteration, allowing angles of attack up to seven degrees) in airborne state*

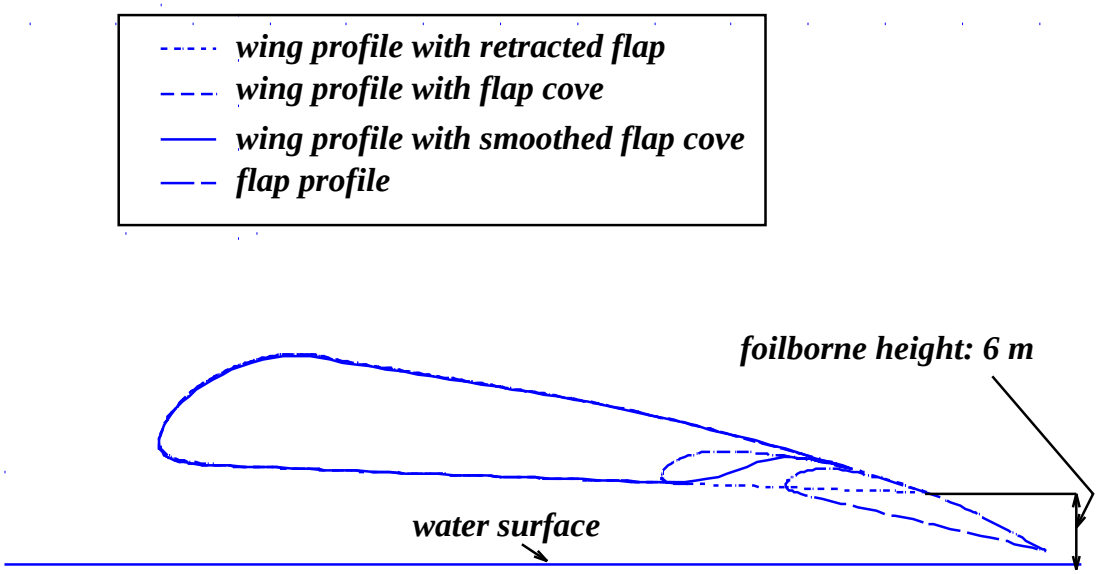

Figure 7: *The wing profile (of earlier design iteration) and the trailing edge flap profile in foilborne state*

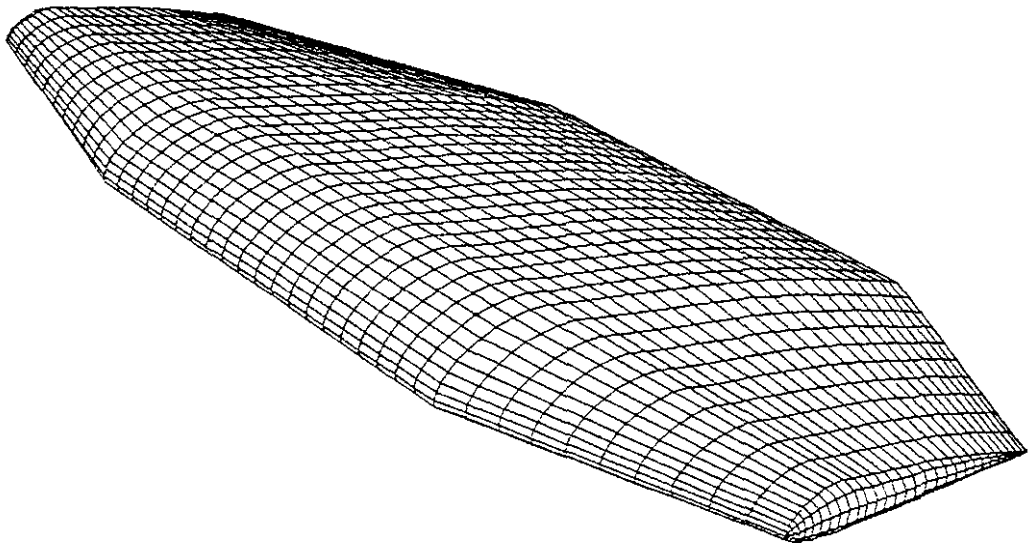

Figure 8: *Panel distribution over the wing*

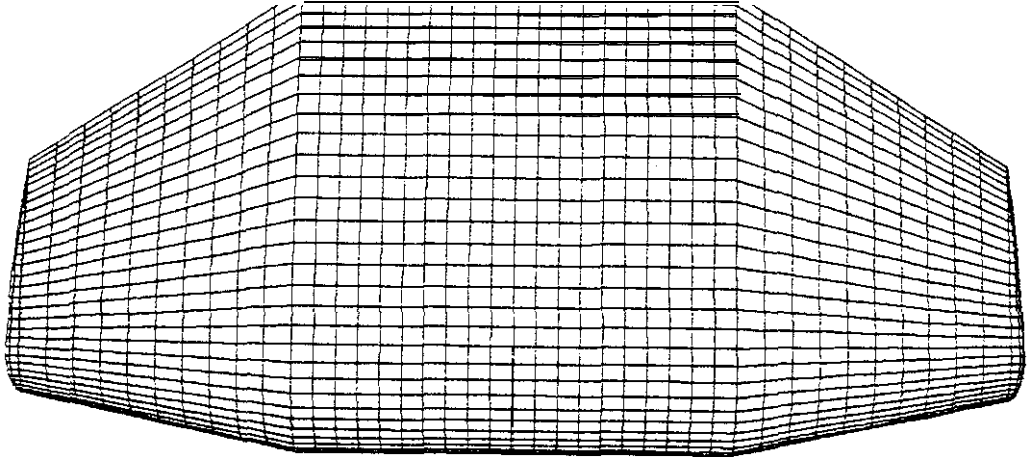

Figure 9: *Panel distribution over the wing; top view*

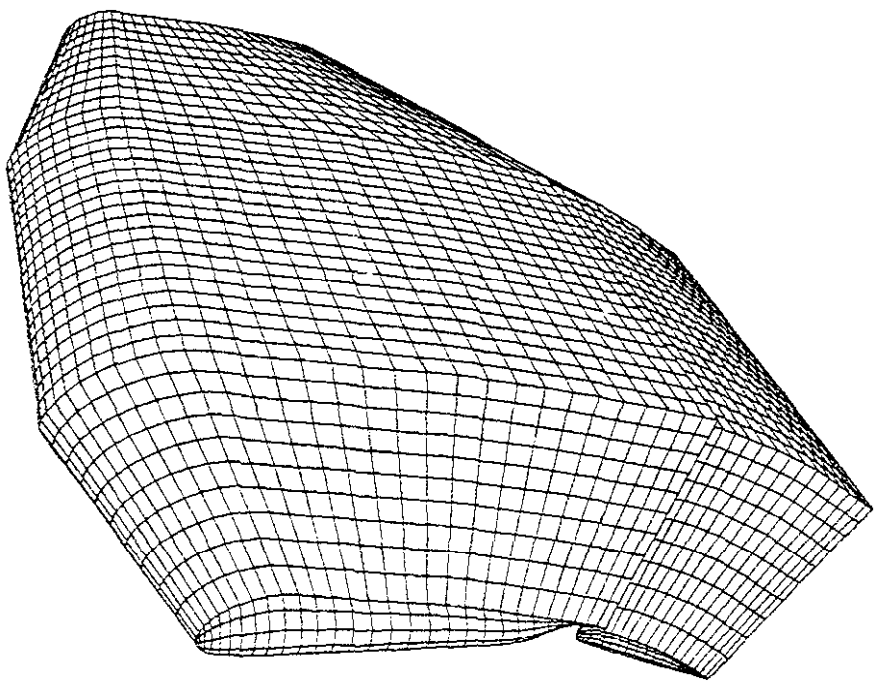

Figure 10: *Panel distribution over the wing with deflected flap*

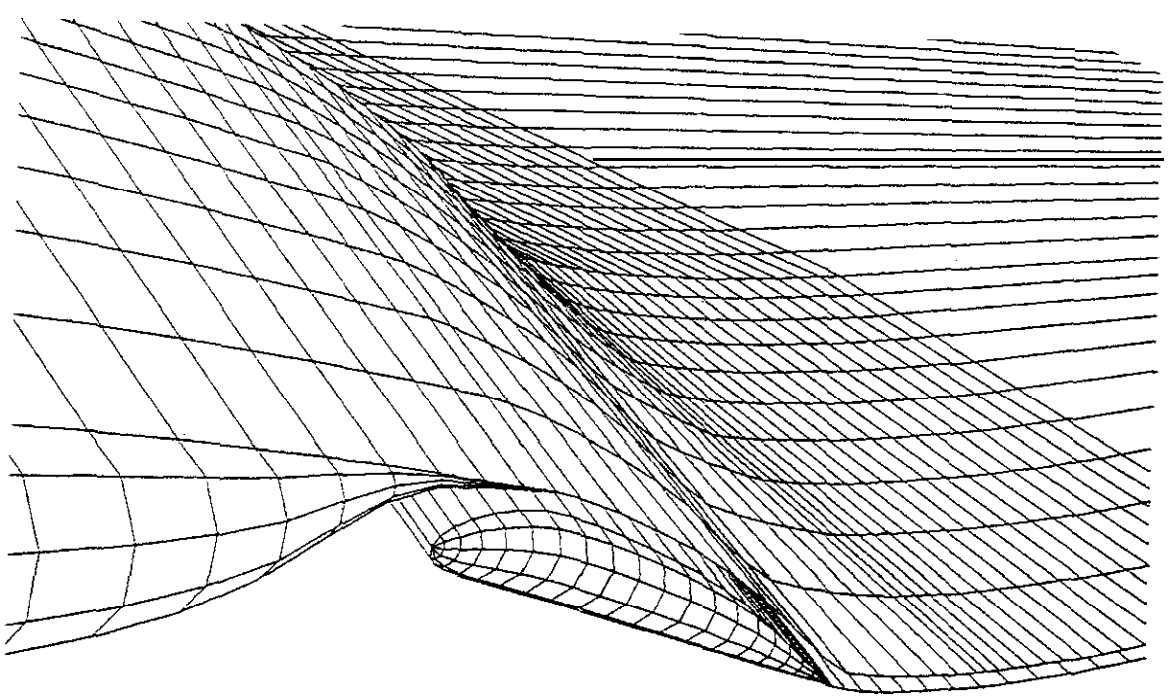

Figure 11: *Panel distribution over the wing with deflected flap and the wakes; detail near the flap*

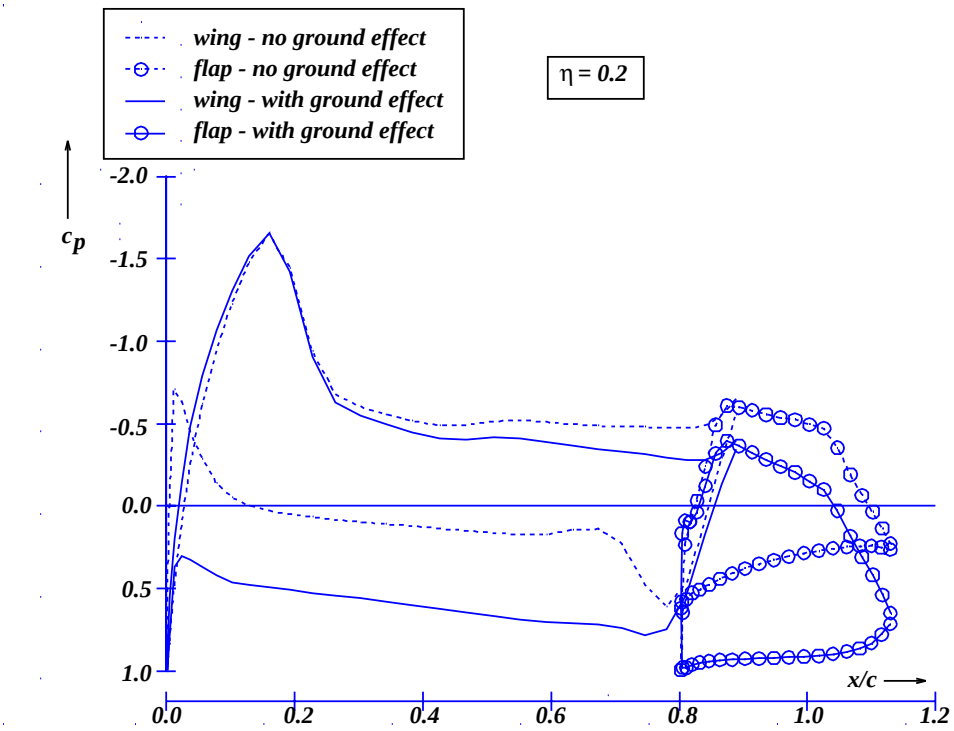

Figure 12: *Pressure distributions over the wing and flap at* $\eta = 0.2$ *for* $U_\infty = 50kts, \alpha = 0°, \delta_f = 15°$, *foilborne state*

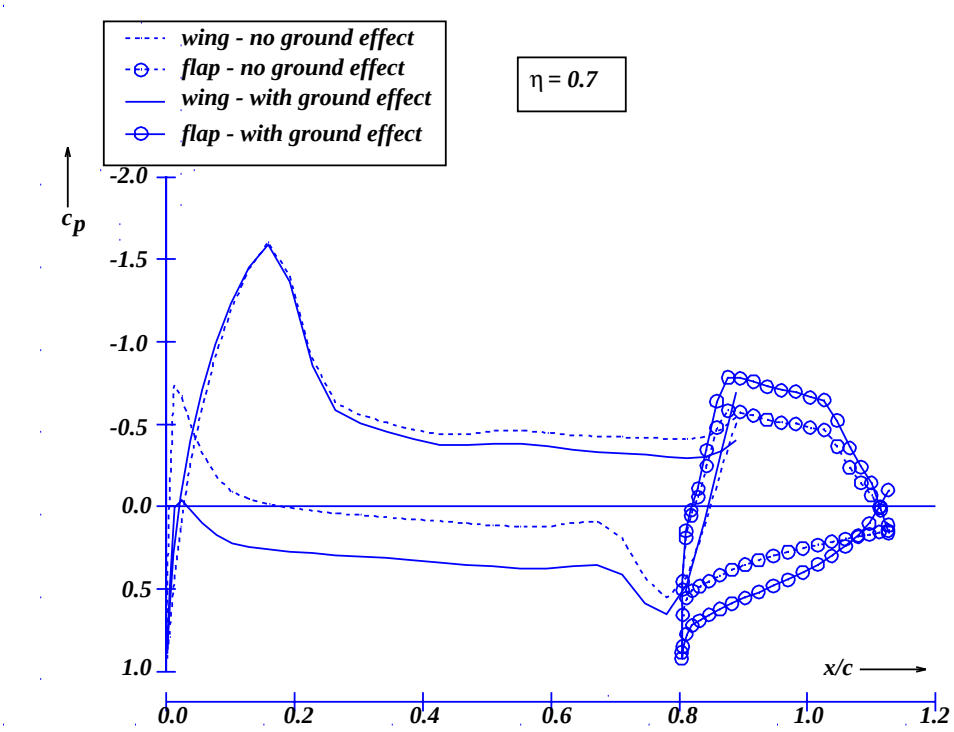

Figure 13: *Pressure distributions over the wing and flap at* $\eta = 0.7$ *for* $U_\infty = 50kts, \alpha = 0°, \delta_f = 15°$, *foilborne state*

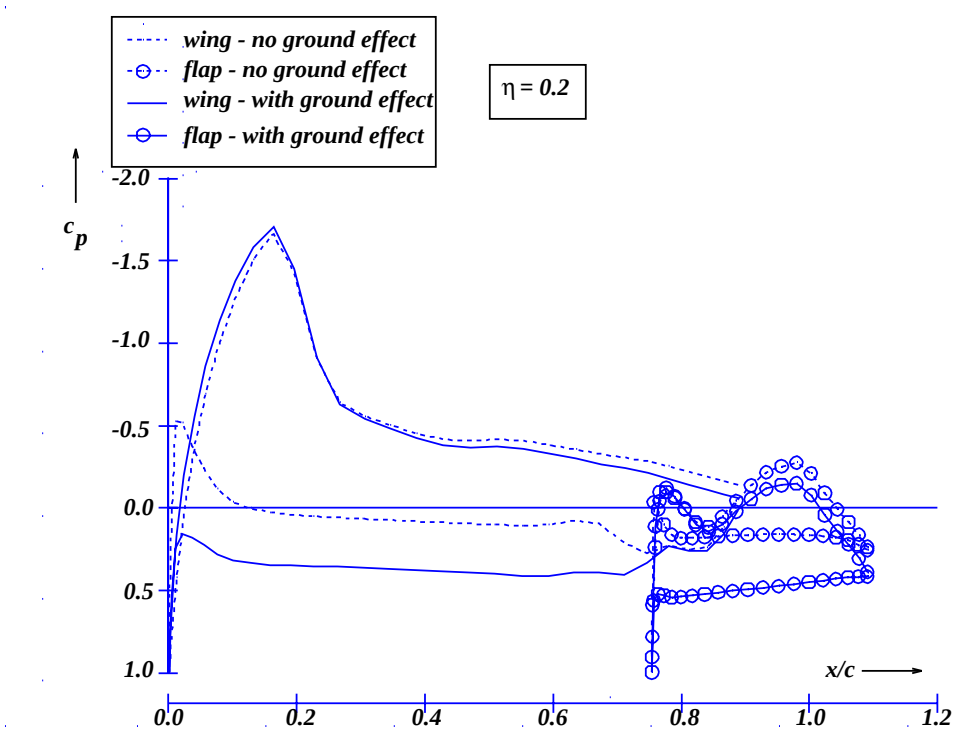

Figure 14: *Pressure distributions over the wing and flap at* $\eta = 0.2$ *for* $U_\infty = 85kts, \alpha = 2.1°, \delta_f = 5°$, *airborne state*

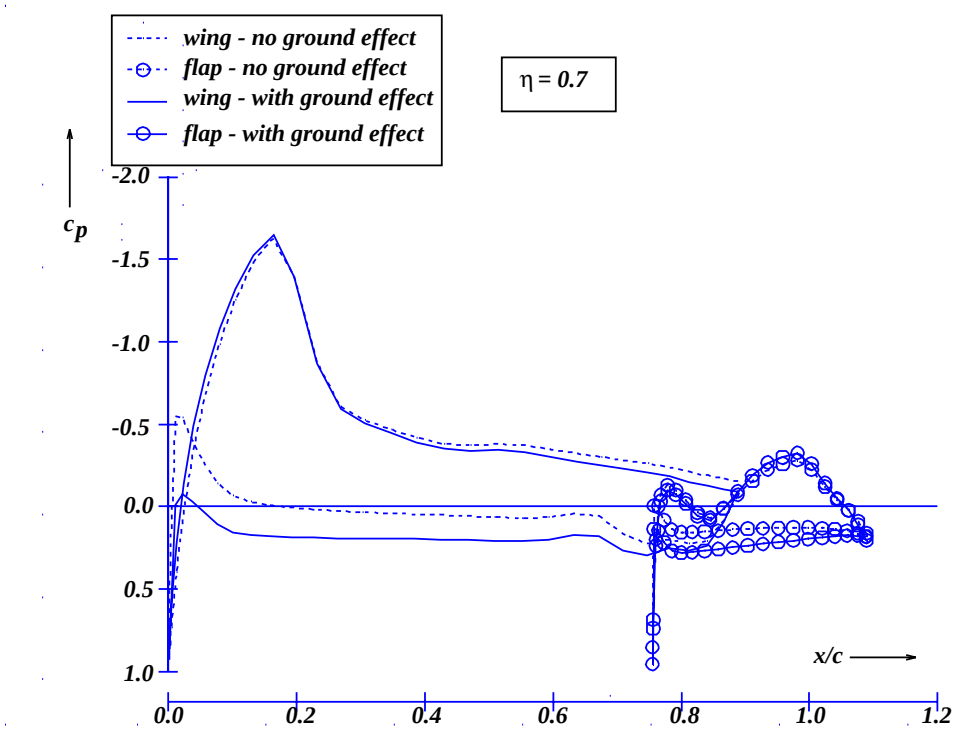

Figure 15: *Pressure distributions over the wing and flap at* $\eta = 0.7$ *for* $U_\infty = 85kts, \alpha = 2.1°, \delta_f = 5°$, *airborne state*

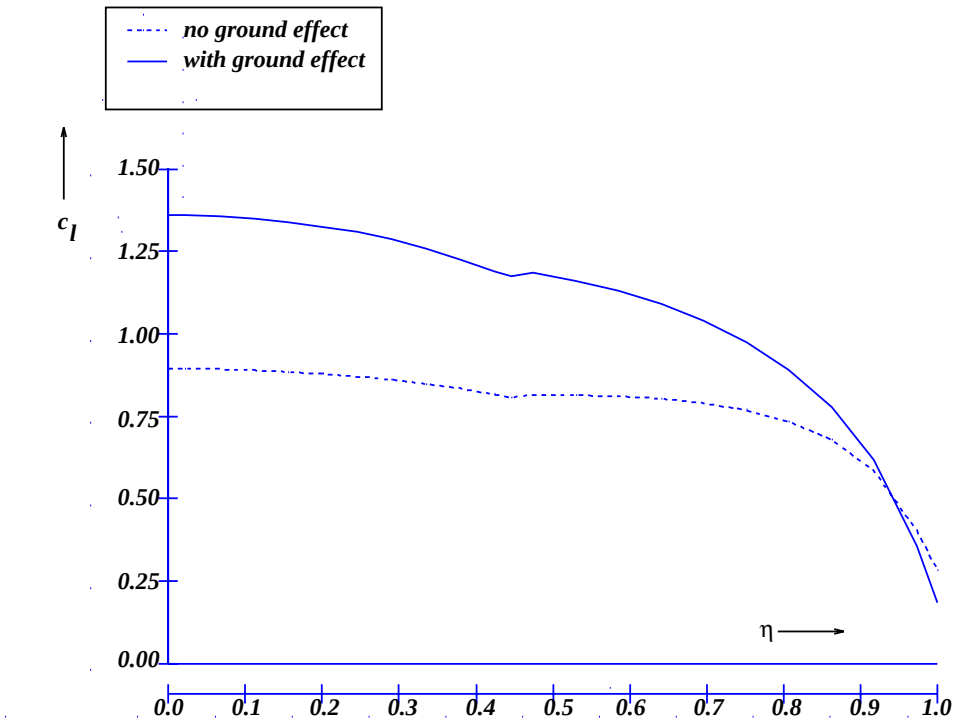

Figure 16: *Spanwise lift distribution over the wing for* $U_\infty = 50kts, \alpha = 0°, \delta_f = 15°$*, foilborne state*

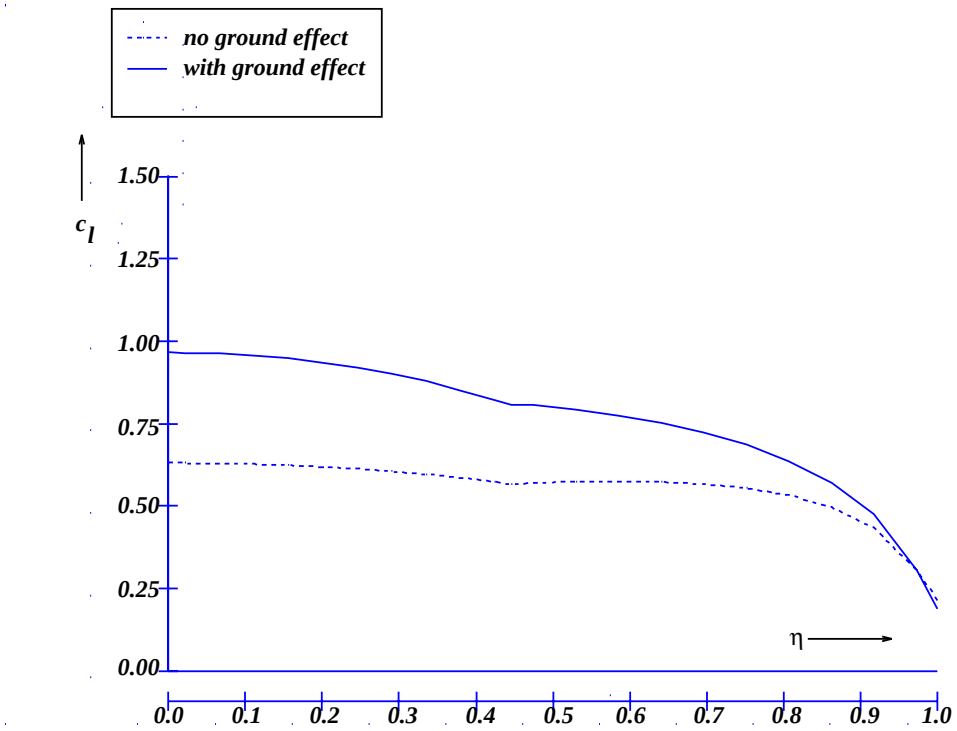

Figure 17: *Spanwise lift distribution over the wing for* $U_\infty = 85kts, \alpha = 2.1°, \delta_f = 5°$*, airborne state*

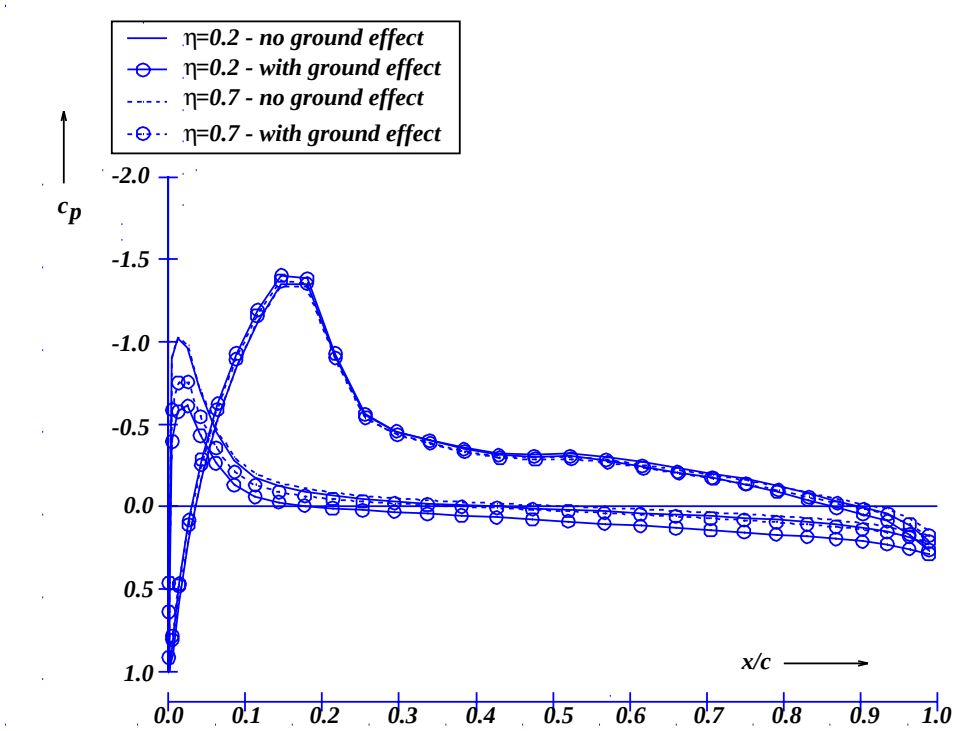

Figure 18: *Pressure distributions over the wing at* $\eta = 0.2$ *and* $\eta = 0.7$ *for* $U_\infty = 120kts, \alpha = 0°, \delta_f = 0°$*, airborne state*

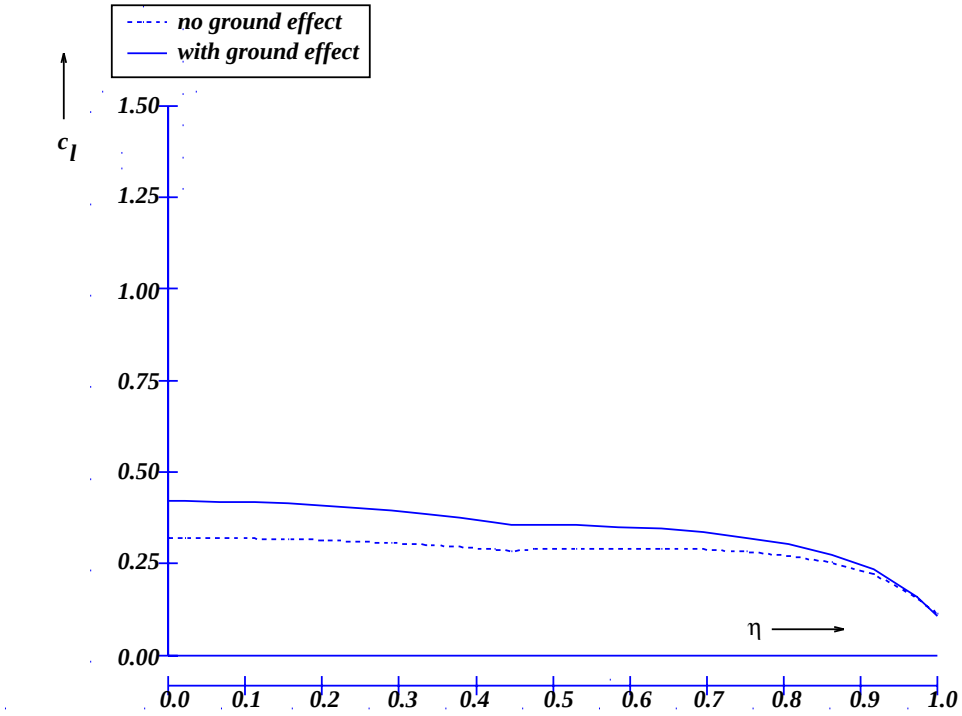

Figure 19: *Spanwise lift distribution over the wing for* $U_\infty = 120kts, \alpha = 0°, \delta_f = 0°$*, airborne state*